11th World Congress on Computational Mechanics (WCCM XI)
5th European Conference on Computational Mechanics (ECCM V)
6th European Conference on Computational Fluid Dynamics (ECFD VI)
E. Oñate, J. Oliver and A. Huerta (Eds)

A POSTERIORI ERROR CONTROL FOR BEM IN 2D-ACOUSTICS

Marc BAKRY*, **Sébastien PERNET**†

* Organisme National d'Etudes et de Recherche Aérospatiale (ONERA/DTIM/M2SN)
2 avenue Edouard Belin, FR-31055 TOULOUSE Cedex 4

POEMS (UMR 7231 CNRS-INRIA-ENSTA)
828, Boulevard des Maréchaux, FR-91762 PALAISEAU Cedex

e-mail: marc.bakry@onera.fr

†Organisme National d'Etudes et de Recherche Aérospatiale (ONERA/DTIM/M2SN)
2 avenue Edouard Belin, FR-31055 TOULOUSE Cedex 4

email: sebastien.pernet@onera.fr

Key words: 2D-acoustics, boundary integral equations, BEM, *a posteriori* error estimate, adaptative refinement

Abstract. We study the efficiency of four different *a posteriori* error estimates for the single layer potential associated with the Helmoltz equation. We show that we obtain the theoretical convergence rates for regular solutions and that adaptative refinement techniques allows to approach them in the case of singular solutions. We also try to evaluate the efficiency constants for some test cases.

1 INTRODUCTION

The main advantage of the Boundary Element Method (BEM), based on boundary integral formulations, is to reduce the discretization to the boundary of the domain and intrinsicaly take into account the radiation conditions at infinity at the cost of the manipultion of fully-populated matrices, thus limiting its use for large-scale applications. Recent improvement on the acceleration of the BEM like the Fast Multipole Method allowed to overcome these difficulties. However, in the context of wave propagation and oscillating kernels, the BEM lacks reliable, efficient, automatic tools for the control of the error. The aim of our work is the study of different *a posteriori* error estimates in the context of the BEM for 2D-acoustics. An error estimate is a tool giving a numerical value η equivalent

to $\|e\|_{\mathrm{H}} = \|p - p_h\|_{\mathrm{H}}$ ($\|.\|_{\mathrm{H}}$ is the norm associated with the space H where p lives),

$$\exists\,(C_1, C_2) > 0,\ C_1\eta \leq \|e\|_{\mathrm{H}} \leq C_2\eta. \tag{1}$$

The error indicator η depends only on the numerical solution and the inputs (frequency, etc.). The left and right inequalities are respectively called *efficiency* and *reliability*. In order to be used in an adaptative refinement algorithm, such estimates must have *local* properties, i.e. one must be able to define $\mu(\tau)$, τ being an element of the discretized domain, such that $\mu(\tau)$ gives some informations about the local error on τ. An example of autoadaptative algorithm is

WHILE "stop criterion not respected"
  calculate solution
  calculate local estimate
  sort the cells
  mark cells following a specific criterion
  remesh with true geometry
END WHILE

This paper will present some preliminary results in acoustics in the case of the *sound-soft* problem (we set a Dirichlet condition on the boundary). We want to solve the Helmoltz equation in an exterior domain Ω with boundary Γ and Radiation Condition (RC) for an incident wave U_{i}

$$\begin{cases} \Delta U + k_{\mathrm{w}}^2 U = 0 & \text{in } \Omega, \\ U = -U_{\mathrm{i}} & \text{on } \Gamma, \\ \text{Sommerfeld RC} \end{cases} \tag{2}$$

We solve this problem using the Single Layer Potential operator SL_k with the unknown $p = \left[\frac{\partial U}{\partial n}\right]$ (jump over gamma of the normal derivative of U)

$$\begin{cases} \mathrm{SL}_{k_{\mathrm{w}}} : \mathrm{H}^{-1/2}(\Gamma) \longrightarrow \mathrm{H}^{1/2}(\Gamma) \\ \qquad\qquad p \longmapsto \displaystyle\int_\Gamma G_k(x,y)\, p(y) d\sigma(y) \\ \qquad G_k(x,y) = \dfrac{i}{4} H_0^{(1)}\left(k_{\mathrm{w}}\,|x-y|\right),\ x \neq y \end{cases} \tag{3}$$

where we denote by $H_0^{(1)}$ the Hankel function of the first kind. The variational formulation is then for any $p' \in \mathrm{H}^{-1/2}(\Gamma)$

$$< \mathrm{SL}_{k_{\mathrm{w}}} p, p' > = < -U_i, p' > = < f, p' > . \tag{4}$$

For $k_{\mathrm{w}} > 0, \mathrm{SL}_{k_{\mathrm{w}}}$ is Fredholm and the problem is well-posed. Consequently, for any finite element approximation $\mathrm{V}_h \subset \mathrm{H}^{-1/2}(\Gamma)$, an uniform discrete inf-sup condition holds ie

$$\exists h_0 > 0,\ \forall h \leq h_0,\ \exists \alpha > 0,\quad \inf_{p_h \in \mathrm{V}_h} \sup_{q_h \in \mathrm{V}_h} \frac{|< \mathrm{SL}_{k_{\mathrm{w}}} p_h, q_h >|}{\|p_h\|_{\mathrm{H}^{-\frac{1}{2}}} \|q_h\|_{\mathrm{H}^{-\frac{1}{2}}}} \geq \alpha > 0$$

and the solution p_h is unique. In particular, the finite elment method leads to a quasi-optimal a priori error estimate ie (Cea's Lemma) $\exists C(\Gamma) > 0$ such that

$$\|p - p_h\|_{\mathrm{H}^{-1/2}} \leq C(\Gamma) \inf_{v_h \in \mathrm{V}_h} \|p - v_h\|\|_{\mathrm{H}^{-1/2}}.$$

We consider two kinds of error estimates:

- two space-reconstruction-based estimates (there exists more),
- one residual-based estimate.

In the following part of this paper, we present the estimates which are at this moment tested and explain why they should work, but we do not give any mathematical proof. Then, we give the convergence curves for three different 2D-objects for both uniform and autoadaptative refinement. Finally, we try to evaluate the different efficiency constant.

2 *A POSTERIORI* ERROR ESTIMATES FOR THE BEM

In this part, we present the three different error estimates which have been tested. The first one is a "natural" one since it is based on the computation of the residual. The two others are based on the same principle which is the projection on an enriched approximation space and only differ over the projection operator. In the following, $\mathcal{T}_H$ is the original mesh and $\mathcal{T}_h$ a n-times (n=2) refined mesh of $\mathcal{T}_H$.
As we cannot compute $\|.\|_{\mathrm{H}^{-\frac{1}{2}}}$, we will use the equivalent norm $\|.\|_G$ associated with the operator SL_0 such that $\|p\|_G^2 =< \mathrm{SL}_0 p, p >$.

2.1 Residual-based Error Estimates

We present a residual-based error estimate. This kind of estimate the the advantage of being "closer" to the error since it verifies $\forall v \in \mathrm{H}^{-\frac{1}{2}}(\Gamma)$

$$< \mathrm{SL}_{k_{\mathrm{w}}} e, v >=< r_h, v >= r_h(v) \tag{5}$$

where $r_h = f - \mathrm{SL}_{k_{\mathrm{w}}} p_h$ is the residual of the problem. Since the problem is well posed, there is an $\alpha > 0$ such that, for all v

$$\sup_{w \in \mathrm{H}^{-1/2}(\Gamma)} \frac{| < \mathrm{SL}_{k_{\mathrm{w}}} v, w > |}{\|w\|_{\mathrm{H}^{-1/2}}} \geq \alpha \|v\|_{\mathrm{H}^{-1/2}}$$

Using the continuity of SL_{k_w} and (5) with $v = e = p - p_h$,

$$\alpha\|p - p_h\|^2_{\mathrm{H}^{-1/2}} \leq \sup_{w\in\mathrm{H}^{-1/2}(\Gamma)} |r_h(w)|,$$
$$\beta\|p - p_h\|_{\mathrm{H}^{-1/2}} \geq \sup_{w\in\mathrm{H}^{-1/2}(\Gamma)} \frac{|r_h(w)|}{\|w\|_{\mathrm{H}^{-1/2}}}.$$

As a consequence,

$$\alpha\|p - p_h\|_{\mathrm{H}^{-1/2}} \leq \sup_{w\in\mathrm{H}^{-1/2}(\Gamma)} \frac{|r_h(w)|}{\|w\|_{\mathrm{H}^{-1/2}}} \leq \beta\|p - p_h\|_{\mathrm{H}^{-1/2}}. \tag{6}$$

$\|r_h\|_{\mathrm{H}^{1/2}}$ is an efficient and a reliable natural a posteriori error estimate. The problem lies in the fact that $\|.\|_{\mathrm{H}^{1/2}}$ is hardly computable and is not local.

Carstensen (see [1]) suggested an estimate based on the computation of the **tangential** gradient of the residual. This estimate was designed for the case of the single layer potential associated with the Laplace-equation.
We have

$$r_h = f - \mathrm{SL}_k p_h \tag{7}$$
$$\mu = \|h^{\frac{1}{2}}\nabla_\tau r_h\|_{L^2(\Gamma)} \tag{8}$$
$$\mu^2 = \sum_{\tau\in\mathcal{T}_H} \mu_\tau^2 \tag{9}$$

where $\mu_\tau = \|h^{\frac{1}{2}}\nabla_\tau r_h\|_{L^2(\tau)}$ corresponds to the local error estimate. Requirements for this estimate are the orthogonality of r_h to $\mathcal{P}^0$ and the $\mathrm{H}^1(\Gamma)$-regularity which are true by construction of r_h. We give here a sketch of proof for the *reliability*-inequality.
Using the space-interpolation inequalities,

$$\exists C > 0, \|r_h\|^4_{\mathrm{H}^{\frac{1}{2}}(\Gamma)} \leq C\|r_h\|^2_{L^2(\Gamma)}\|r_h\|^2_{\mathrm{H}^1(\Gamma)}, \tag{10}$$
$$\|r_h\|^4_{\mathrm{H}^{\frac{1}{2}}(\Gamma)} \leq C\|r_h\|^2_{L^2(\Gamma)}\left(\|r_h\|^2_{L^2(\Gamma)} + |r_h|^2_{1,\Gamma}\right).$$

By definition of $\|.\|_{L^2(\Gamma)}$, taking into account that for any $v_h \in \mathcal{P}^0(\Gamma)$, v_h and r_h are orthogonal (it corresponds only to the FEM formulation $\forall v_h, (r_h, v_h) = 0$),

$$\|r_h\|^2_{L^2(\Gamma)} = \int_\Gamma \overline{r_h} r_h d\gamma,$$
$$\|r_h\|^2_{L^2(\Gamma)} = \int_\Gamma \overline{r_h}(r_h - v_h) d\gamma.$$

Applying the Cauchy-Schwartz inequality,

$$\|r_h\|^2_{L^2(\Gamma)} \leq \inf_{v_h\in\mathcal{P}^0(\Gamma)} \|r_h - v_h\|_{L^2(\Gamma)}\|r_h\|_{L^2(\Gamma)}.$$

Let $\mathrm{I}_h r_h$ be any $\mathcal{P}^0$-interpolation of the residual, using the Bramble-Hilbert lemma (see [3]),

$$\|r_h\|_{L^2(\Gamma)} \leq \|r_h - \mathrm{I}_h r_h\|_{L^2(\Gamma)}$$
$$\|r_h\|_{L^2(\Gamma)} \leq C_1 h \left|r_h\right|_{1,\Gamma}.$$

We apply the previous result to (10)

$$\|r_h\|^4_{\mathrm{H}^{\frac{1}{2}}(\Gamma)} \leq \underbrace{C_2 h^4 \left|r_h\right|^4_{1,\Gamma}}_{o(h^2|r_h|^4_{1,\Gamma})} + C_3 h^2 \left|r_h\right|^4_{1,\Gamma}$$

and get the required result

$$\|r_h\|_{\mathrm{H}^{\frac{1}{2}}(\Gamma)} \leq C_5 h^{1/2} \left|r_h\right|_{1,\Gamma}. \tag{11}$$

The main advantage of this estimate is that it does not require the computation of p_h on a finer mesh, thus avoiding the manipulation of bigger fully-populated matrices. Unfortunately, the computation of the norm of the gradient of the residual requires the numerical integration of singularities. The singular part of SL_k is integrated analytically and the smooth part is integrated numerically. The computation is performed by QUADPACK. This process can take some time as the size of the problem increases.

2.2 Space-Reconstruction-based Error Estimates

This estimate is based on the work of Carstensen and Praetorius (see [2]) where it was established for the Laplace equation. It is based on the computation of a solution on $\mathcal{T}_h$ with a polynomial approximation space $\mathcal{P}^k(\mathcal{T}_h)$ (in our case $k = 0$). This solution is reconstructed on a "richer" approximation space $\mathcal{P}^{k'>k}(\mathcal{T}_H)$ ($k' = 1$) and the norm of their difference is calculated. The estimator is build through the following steps

- Consider some projection operator Π. Π can refer either to a standard L^2-projection (Π_{L^2}) operator or the projection operator associated with the "energy"-norm $\|.\|_G$ (Π_G) on $\mathcal{P}^{k'>k}(\mathcal{T}_H)$. In this case one must pay attention to the fact that, since we are using the single-layer potential associated with the Laplace-equation in two dimensions, it is not invertible for objects of capacity equal to 1 (see [4]): circle with radius $R = 1$, square with side $a = 1.69$, etc. In particular the projection operator degenerates as $\mathcal{T}_H$ gets finer and $\|.\|_G$ is not a norm anymore.
  We use Π to project $p_h \in \mathcal{P}^0(\mathcal{T}_h)$ on $\mathcal{P}^1(\mathcal{T}_H)$. One can show under certain regularity conditions on p (p is regular "enough") that

$$p - p_h = \underbrace{p - \Pi p}_{o(\Pi p_h - p_h)} + \underbrace{\Pi(p - p_h)}_{o(\Pi p_h - p_h)} + \Pi p_h - p_h \tag{12}$$

  such that in the end

$$\|p - p_h\|_G \sim \|\Pi p_h - p_h\|_G. \tag{13}$$

- Once the projected solution is calculated, an estimation of the overall error is given by simple computation of $\|\Pi p_h - p_h\|_G$.
- The last step is to *localize* the error. Standard localization pattern provide an overall error estimate

$$\|\Pi p_h - p_h\|_G \sim \|H^{\frac{1}{2}} (\Pi p_h - p_h)\|_{L^2(\Gamma)} \tag{14}$$

where H is the length of an element $\tau \in \mathcal{T}_H$. Furthermore, we have

$$\|H^{\frac{1}{2}} (\Pi p_h - p_h)\|^2_{L^2(\Gamma)} = \sum_{\tau \in \mathcal{T}_H} \underbrace{\|H^{\frac{1}{2}}(\tau) (\Pi p_h - p_h)\|^2_{L^2(\tau)}}_{\text{local error estimate}}. \tag{15}$$

These estimates have the advantage of being really easily computable. Problems arise for Π_G when the number of degrees of freedom increases since it requires the inversion of a fully-populated matrix. Π_{L^2} also has the advantage of being always computable and only requires the inversion of a sparse matrix.

3 NUMERICAL RESULTS

In the case of a $\mathcal{P}^0$, the best convergence rate which is to be expected is $O(N_{\text{DOF}}^{-3/2})$. When using uniform refinement, this rate is usually bounded above by the regularity of the solution. We consider three different objects enlightened by a plane wave incoming from their right:

- circle with radius $R = 2$. Γ and f being smooth, a smooth solution is to be expected.
- ellipse with major/minor axis $a = 2$ and $b = 0.5$. We expect the same convergence rate as for the circle.
- square with side $a = 1$. There is an ingoing singularity of Γ in Ω at the edges of the square. Consequently, there is no reason to expect a smooth solution as singularities of the solution are expected on the edges.

We choose $k_{\text{w}} = 10$ in order to start with a low amount of degrees of freedom (DOF). We calculate the three estimates mentioned above and the "exact" error in order to compute the efficiency constants (see Part 4 for more details on the computation of e_{exact}). Curves are given for both uniform and autoadaptative refinement. Autoadaptative refinement is done by using a Dörfler-algorithm (see for example [5]) with parameter $\theta = 0.5$. We give a quick reminder of the principle. We try to find the minimal ensemble $\mathcal{M}(\mathcal{T}_H)$ (ie the minimal ensemble of elements of $\mathcal{T}_h$ to be remeshed) such that

$$\theta \sum_{\tau \in \mathcal{T}_H} \mu_\tau^2 \leq \sum_{\tau \in \mathcal{M}(\mathcal{T}_H)} \mu_\tau^2.$$

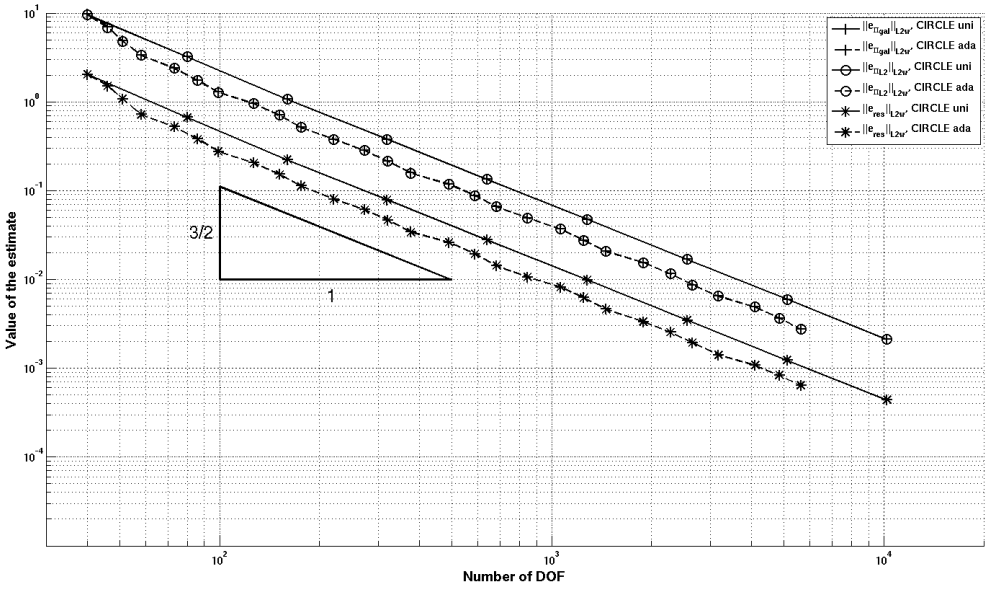

Figure 1: Convergence of the different estimates for both uniform and autoadaptative mesh-refinement, circle with radius $R = 2$.

We base the local estimation on the localization of the Π_{L^2}-based estimate. We stress that the other estimates (Π_G and residual-based) behave equivalently. The elements which are refined are cut in two equivalent elements, and the new node is projected on the true surface of the object.

3.1 Circle and Ellipse

We show in Fig. 1 and Fig. 2 the values of the different estimates for both the circle and the ellipse for uniform and autoadaptative mesh-refinement.

We observe that the $O(N_{\text{DOF}}^{-3/2})$-convergence rate is reached. Consequently, the autoadaptative refinement has only little influence. A really good point is that the estimates seem to behave as expected.

3.2 Square

The case of the square is a bit more complicated. Contrary to the two test cases above, the singularities in the solution prevent from reaching the optimal convergence rate in uniform refinement. The estimate convergence is represented in Fig. 3.

One can see that the uniform convergence rate is 2/3. The use of an autoadaptative algorithm allows to reach the optimal convergence rate. Looking at Fig. 4, we observe that the algorithm refined a lot around the edges of the square where the solution is, as expected, singular. The view seems to be 3D, but it is **a 2D-mesh which is artificially**

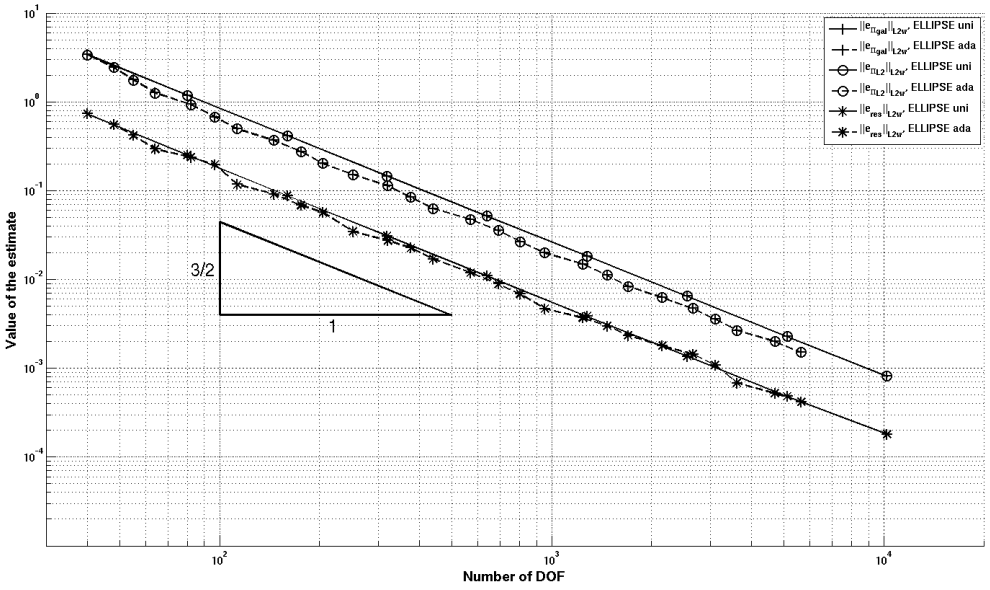

Figure 2: Convergence of the different estimates for both uniform and autoadaptative mesh-refinement, circle with major/minor axis $a = 2$ and $b = 0.5$.

transformed into a 3D-mesh to see clearly the colors which means that the 2D-segments are represented by 3D-rectangles.

Testing on other geometries (not presented here) which are not smooth nor symmetrical, the three estimates behave the same way, which is an encouraging point.

4 EFFICIENCY CONSTANTS

We try now to estimate the values of some characteristic constants for the reconstruction-based estimates and the "localization" constants of the norms, i.e.

- the ratios $\|.\|_{\mathrm{G}}/\|H^{1/2}(.)\|_{L^2}$ for the reconstruction based estimates and the exact error,
- the ratios $\|e_{\mathrm{exact}}\|_{\mathrm{G}}/\|e_{\Pi_{\mathrm{gal}}}\|_{\mathrm{G}}$ and $\|e_{\mathrm{exact}}\|_{\mathrm{G}}/\|e_{\Pi_{L^2}}\|_{\mathrm{G}}$ which are nothing else than the efficiency constants.

We explain now how e_{exact} is computed. We first calculate a solution on a really accurate and uniform mesh in $\mathcal{P}^1(\mathcal{T}_H)$. In our case, $\mathrm{card}(\mathcal{T}_H) = 10240 = 40.2^8$ which corresponds to 9 iterations with uniform refinement and an initial mesh of size 40. In order to compute the solution, we try for each node of the current mesh to find the corresponding node in the accurate mesh. It is then easy to compute the solution. In this case, one immediately see that it is not possible to use this "solution" as basis for a comparison in the case of autoadaptative refinement. If we take the case of the square, the edge-cells will be

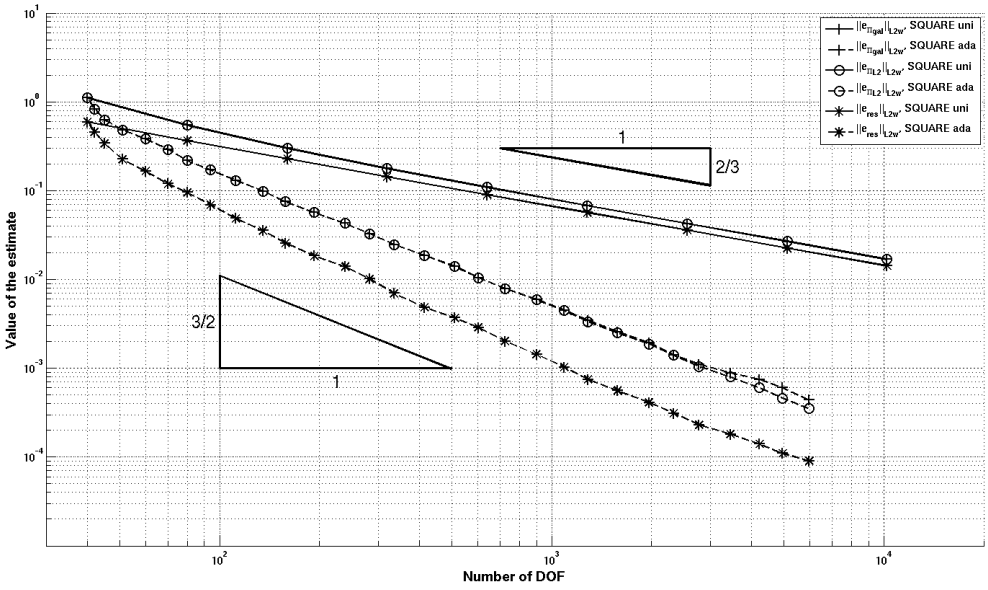

Figure 3: Convergence of the different estimates for both uniform and autoadaptative mesh-refinement, square with side $a = 1$.

systematically refined. After 9 iterations, the cell size at the edge with an autoadaptative strategy is exactly the same as in the reference mesh. On the 10^{th}, the cells will be two times smaller, what does not make sense anymore. As a consequence we only present results involving the computation of e_{exact} for an uniform refinement strategy.
We present in Fig. 5 the "localization" constants. These constants depend as expected only on the geometry and (after stabilization) not on the number of DOF.

From (12), the efficiency constant should be around 1 for sufficiently regular-shaped objects. We can see on Fig. 6 that this is the case since the constants for the ellipse and the circle are around 1 but not for the square.

5 CONCLUSION

The three presented error estimates prove to be valid tools for the use of autoadaptative refinement techniques. They behave as expected for different kind of solutions and geometry. The next development will be to test another estimate based on the local inversion of the error/residual equation (5) and/or use a different kind of incoming wave, like a dipole. We also want to check their characteristics as the frequency increases. The previous preliminary results show that the Π_{L^2}-based error estimate is a good, fast and reliable candidate.

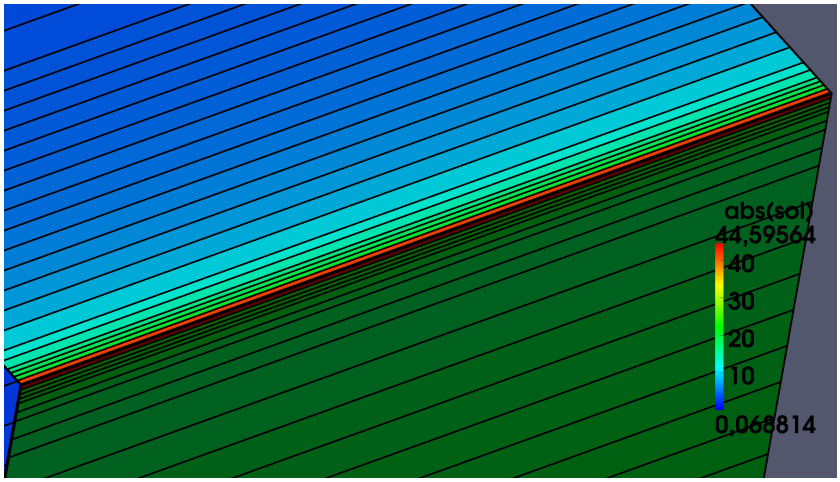

Figure 4: Detailed view of the top right edge of the square after 5 iterations and $\theta = 0.5$. The algorithm "captures" the singularity on the edge (represented value is the modulus of p_h on the square).

6 ACKNOWLEDGEMENTS

This work is funded by the *Agence Nationale de la Recherche* and by the *Ministère français de la Défense - Direction Générale de l'Armement*.

REFERENCES

[1] C. Carstensen *An a posteriori error estimate for a first-kind integral equation*. Mathematics of Computation, Vol. 66, No. 217, 1997, pp. 139-155.

[2] C. Carstensen, D. Praetorius, *Averaging techniques for the effective numerical solution of Symm's integral equation of the first kind*. SIAM J. Sci. Comput., Vol. 27, No. 4, 2006, pp. 1226-1260

[3] P.G. Ciarlet, *The finite element method for elliptic problems*. SIAM, Classics of Applied Mathematics Vol. 40, 1978.

[4] W. Dijkstra, *Condition Numbers in the Boundary Element Method: Shape and Solvability*. Tech. University Eindhoven, 2008.

[5] M. Feischl, M. Karkulik, J.M. Melenk, D. Praetorius, *Quasi-optimal convergence rate for an adaptative boundary element method*. TU Wien, ASC Report No. 28/2011, 2011.

[6] W. McLean, *Strongly Elliptic Systems and Boundary Integral Equations*. Cambridge University Press, 2000.

[7] J.C. Nédélec, *Acoustic and Electromagnetic Equations, Integral Representations for Harmonic Problems*. Springer, Applied Mathematical Sciences Vol. 144., 2001.

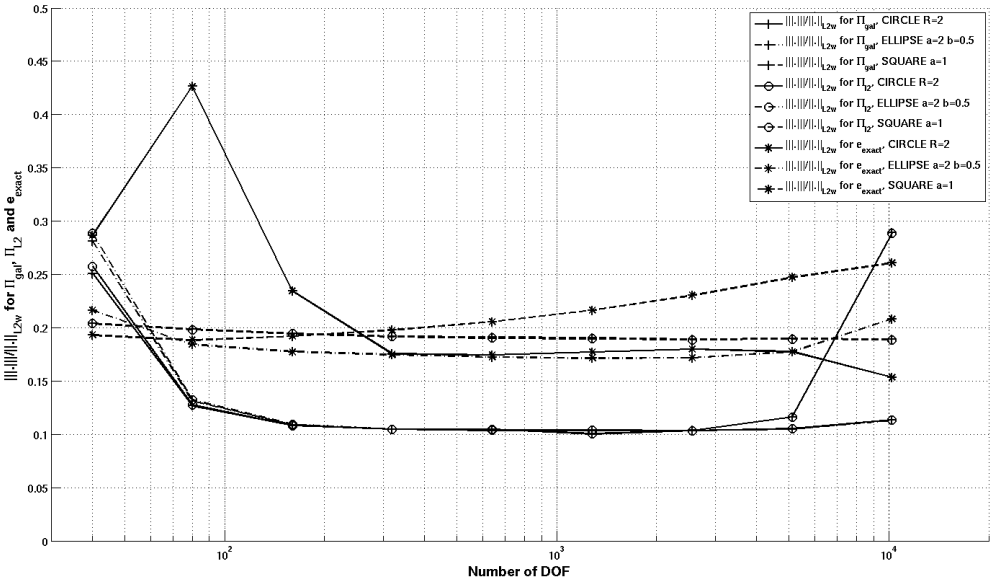

Figure 5: Localization constants for e_{exact}, $e_{\Pi_{\text{gal}}}$ and $e_{\Pi_{L^2}}$ for the circle, the ellipse and the square.

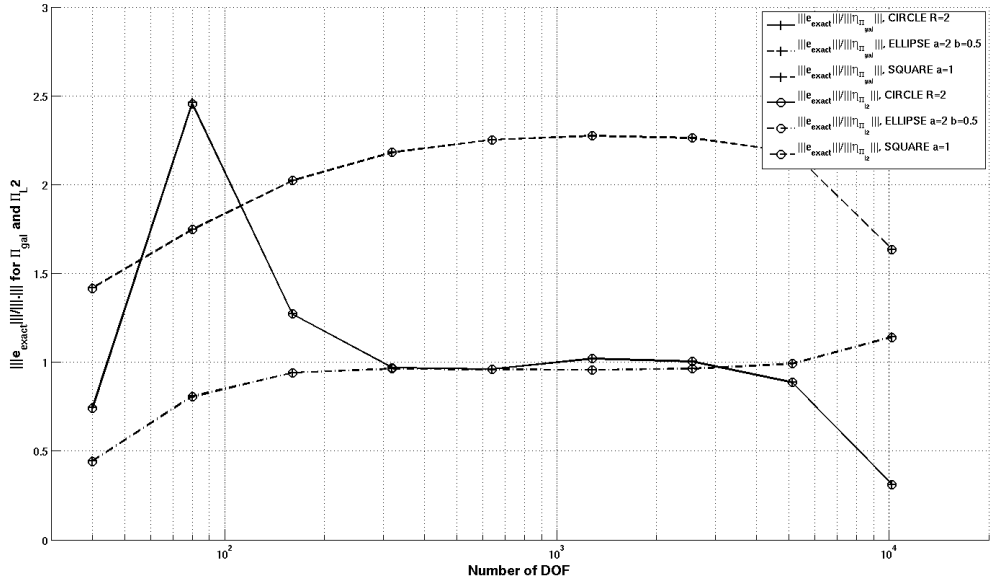

Figure 6: Efficiency constants for the circle, the ellipse and the square.